

# Structural and Magnetic Study of $\text{BaLa}_x\text{Fe}_{12-x}\text{O}_{19}$ Nanohexaferrites Synthesized via Sol–Gel Auto-Combustion Technique

Shanker Lal<sup>1</sup>, Rajesh Kumar Gupta<sup>2</sup>, Sarvesh Narain Asthana<sup>3</sup>, D. K. Sahu<sup>4</sup>

<sup>1</sup>Department of Physics, Accurate Institute of Management and Technology, Gr. Noida (U.P.)-201301, India

<sup>2</sup>Department of Physics, Dr. Ambedkar Institute of Technology for Divyangjan, Kanpur (U.P.)-208024, India

<sup>3</sup>Department of Physics, Bipin Bihari College, Jhansi (U.P.)-284001, India

<sup>4</sup>Department of Physics, R.S. Government P.G. College, Lalitpur (U.P.)-284402, India

**Abstract--** The sample of M-type barium hexaferrites of general formula  $\text{BaLa}_x\text{Fe}_{12-x}\text{O}_{19}$ , where  $x = 0.0, 0.4, 0.8, 1.2$  have been prepared using Sol-gel auto combustion method. The structural, micro structural and magnetic properties analysis has been done by (XRD), Transmission Electron Microscope (TEM), Scanning electron microscope (SEM), and vibrating sample magnetometer (VSM). XRD data in our study shows that the prepared samples have hexagonal structure. The crystal size was in the range of 30–50 nm and increases with the increasing substitution of  $\text{La}^{3+}$  ions. SEM micrographs show homogeneous distribution of grains with hexagonal morphology. TEM images confirm nanosize of prepared samples. FTIR spectrum confirmed that bands in the range 500–600  $\text{cm}^{-1}$  confirm the formation of Hexaferrite. The significant increase in saturation magnetization increase in observed with the increase in  $\text{La}^{3+}$  substitution.

**Keywords--** M-type Nanohexaferrite, Magnetic properties, Saturation magnetization, Sol-gel Auto combustion, XRD.

## I. INTRODUCTION

The interesting functional properties of hexaferrites make them most innovative class of ferrites. These hexaferrites have high uniaxial magneto crystalline anisotropy [1-2], low microwave losses, narrow FMR line width, low values of eddy current losses, and also self-biasing nature. Such interesting properties make these material solutions for application in microwave and millimetre devices.

M-type hexagonal ferrites have Magnetoplumbite structure with molecular  $\text{MFe}_{12}\text{O}_{19}$  ( $\text{M} = \text{Ba}, \text{Sr}, \text{Pb}$ ) and  $\text{P6}_3/\text{mmc}$  (No 194) space group [3]. Crystal structure of M-type  $\text{BaFe}_{12}\text{O}_{19}$  contains two stacking layers, one is of closed oxygen and other barium layers along the hexagonal  $c$ -axis with basic blocks: Spinel" block (S), Hexagonal (R) with sequence  $\text{RSR}^*\text{S}^*$ . Here,  $\text{S}^*$  and  $\text{R}^*$  have equal number of atoms similar as S and R blocks and its rotation is at  $180^\circ$  along  $c$ -axis.

The crystal structure of M-Type hexagonal ferrite consists of 64 ions per hexagonal unit cell on different eleven basis sites. The 24  $\text{Fe}^{3+}$  ions are distributed on five distinct crystallographic sites. There five sites have one tetrahedral site ( $4f_1$ ) three octahedral sites ( $12k, 2a, 4f_2$ ), and one trigonal bipyramidal site (2b) which is also according to Groter Model [4]. There are several methods for synthesis of barium hexaferrite nanoparticles includes solid state reaction [5], microemulsion method [6] coprecipitation method [7] sol gel [8] ceramic method [9]. In present work, barium hexaferrite nanoparticles are synthesized using auto –combustion method.

The auto combustion method is a sol gel reaction process containing exothermic process of self combustion of oxidant/precursor materials. Advantage of this method is that, nanoparticles formed are of uniform size distribution, easy process, low sintering temperature etc. The  $M_s$  value of 77.188 emu/g and  $H_c = 4324\text{Oe}$  was obtained for Barium hexaferrite samples of pure as well as  $\text{La}^{3+}$  ion doped samples. They have not found perfect hysteresis curves. As we can see from literature review, the structural, micro structural and magnetic properties of substituted Barium hexaferrites are studied by most of the researchers, but the available research data on rare earth  $\text{La}^{3+}$  doped M-type nanohexaferrites is less attempted.

So, due to technological application of M-type Barium hexaferrites, we have examined the substitution effects of  $\text{La}^{3+}$  ions on the structural, microstructural and magnetic properties of sol–gel auto combustion synthesized nanosize  $\text{BaFe}_{12}\text{O}_{19}$  hexaferrites.

We have prepared our Barium ferrite samples using Sol-gel auto combustion method; because this provides good control over particle size and easy process. The main focus of this research work is to synthesis of rare earth La ion doped nanosize Barium hexaferrites with chemical formula  $\text{BaLa}_x\text{Fe}_{12-x}\text{O}_{19}$  ( $x = 0.0, 0.4, 0.8, 1.2$ ). After preparing all samples, they have been investigated for determination their structure, morphology and magnetic properties.

## II. EXPERIMENTAL SETUP

### A. Sample Preparation

La<sup>3+</sup> ion substituted M-type barium Hexaferrites BaLa<sub>x</sub>Fe<sub>12-x</sub>O<sub>19</sub> with the concentration of x = 0.0, 0.4, 0.8 and 1.2 have been synthesized by Sol-gel auto combustion method. The starting materials have been taken of laboratory grade Ba (NO<sub>3</sub>).4H<sub>2</sub>O, La(NO<sub>3</sub>)<sub>3</sub>.9H<sub>2</sub>O, Fe(NO<sub>3</sub>)<sub>3</sub>.9H<sub>2</sub>O, NH<sub>2</sub>CONH<sub>2</sub> and dissolved in unionized distilled water heated at 80°C temperature on hot plate up to 3 hours. Urea gives required energy to initiate exothermic reaction. After heating, the solution of all nitrates becomes brown colour gel. This gel was then kept in digitally controlled microwave oven and was fired to obtain the fine powder (ash) of samples. The ash was then collected and grinded in Pestel mortar for 5 hours to get ultra-fine homogeneous powder of samples. The sample was then sintered in muffle furnace up to 800<sup>0</sup> C for about 5 h by increasing the temperature slowly (100<sup>0</sup> C/h) and then cooled at the same rate. Finally the sample was again grinded in Pestel mortar for then sintered in muffle furnace up to 800<sup>0</sup>C for about 5 h by increasing the temperature slowly (100<sup>0</sup> C/h) and then cooled at the same rate. Finally the sample was again grinded in Pestel mortar for about an hour. These final powders samples so produced are then kept in humidity free atmosphere in air tight bottles for further characterizations.

### B. Characterization Techniques

The crystal structural and phase determination has been done by X-ray diffraction technique using model Bruker AXS D8 Advance diffractometer using source Cu- $\alpha$  radiations. The XRD patterns have been taken in 2 $\theta$  range from 20 to 80° having step size of 0.02°. The analysis of surface morphology has been studied by Scanning Electron Microscopy (FEG-SEM) model JSM-7600F and Transmission electron Microscopy (HR-TEM) FEI, Model Technai G2, F30 of accelerating potential 300kV. Magnetic hysteresis is recorded using vibrating sample magnetometer (LAKESHORE) VSM 7410 Series Model at room temperature.

## III. RESULT AND DISCUSSION

### A. Structural Properties

#### 1) XRD Analysis

The XRD patterns of BaLa<sub>x</sub>Fe<sub>12-x</sub>O<sub>19</sub> hexaferrite powders sintered at 800<sup>0</sup>C for 5h are shown in Fig.1. The intensity and peak position of all diffraction peaks in our work are well matched with the standard powder diffraction file.

The presence of peaks having hkl values such as (008), (110), (107), (114), (203), (217),(201) confirms the hexagonal structure of synthesized samples. This confirms hexagonal phase of the prepared samples with P6<sub>3</sub>/mmc space group. The peak of 100% intensity is observed at (107) plane of barium hexaferrite. In XRD pattern of pure barium sample, we also observed secondary, it may be because of incomplete reaction between reactants, but it disappears in La<sup>3+</sup> ion substituted samples because lanthanum ion has good solubility [10]. From XRD pattern it can also be concluded that doping has not resulted in any formation of secondary phase, it shows homogeneity of the synthesized nano hexaferrite except for pure barium ferrite sample. This shows that all La<sup>3+</sup> doped properly in hexaferrites. Some of the researchers also shows secondary phase with La<sup>3+</sup> ion substitution. After the substitution of La<sup>3+</sup> ions, we observed that there is no crystal structure change and it remains hexagonal structure [11]. All XRD data are given in Tables 1.

The average crystal size of all sample was calculated from the peak position (107), (114) using the Scherer formula [12].

$$D = 0.9 \lambda / \beta \cos\theta \quad (1)$$

Where, D is the crystal size in nm,  $\beta$  is full width at half maximum (FWHM),  $\theta$  is the peak position in radian and  $\lambda$  is the radiation wavelength. The values of lattice parameters and X-ray density of sample was calculated by using the formula given below [13]

$$D_x = 2M/N_A V_{cell} \quad (2)$$

$$\frac{1}{d^2} = \frac{4h^2 + hk + k^2}{3l^2} + \frac{l^2}{c^2} \quad (3)$$

Where, 'd' is lattice spacing and h k l is miller indices.

An increase in the particle size (26.26–50.10 nm), lattice parameter 'a' (5.851–5.893 Å) and 'c' (23.17–23.41 Å) was observed due to La<sup>3+</sup> ion substitution. Similar results were obtained [14]. For sample of x = 1.2, lattice constants 'a' value has maximum value of (5.8939 Å) and value of 'c' varies from 23.17 Å to 23.41 Å . Here, axial ratio (c/a) is almost constant for all samples. The lattice parameters were observed to increase because of the difference in ionic radius of La<sup>3+</sup> (1.15 Å) as compared to that of Fe<sup>3+</sup> (0.67 Å) ions. As La<sup>3+</sup> ions replaced the Fe<sup>3+</sup> ions an internal stress make the lattice distorted and an expansion of the unit cell. From XRD data table1, It is seen that sample BaLa<sub>1.2</sub>Fe<sub>10.8</sub>O<sub>19</sub> have highest volume because of its higher value of lattice constant 'a'.

The density was also observed to increase with the substitution of  $\text{La}^{3+}$  ions it may be occurs due to the volume as well as increase in molecular weight.

Fig. 2 shows the variation of  $\text{La}^{3+}$  ion concentration with X-ray density. As we increase the  $\text{La}^{3+}$  ion substitution, X-ray density also increases.

**Table 1.**  
**Structural data for  $\text{BaLa}_x\text{Fe}_{12-x}\text{O}_{19}$  samples**

Sample content (x)	Lattice parameter		c/a	X-ray Density (Dx) gm/cc	Volume (Vcell) $\text{\AA}^3$	Crystal Size (D) nm
	a ( $\text{\AA}$ )	c ( $\text{\AA}$ )				
0.0	5.851	23.17	3.961	5.370	687.12	26.26
0.4	5.865	23.41	3.991	5.450	697.36	50.10
0.8	5.883	23.32	3.964	5.594	699.20	40.24
1.2	5.893	23.30	3.954	5.737	701.03	33.42

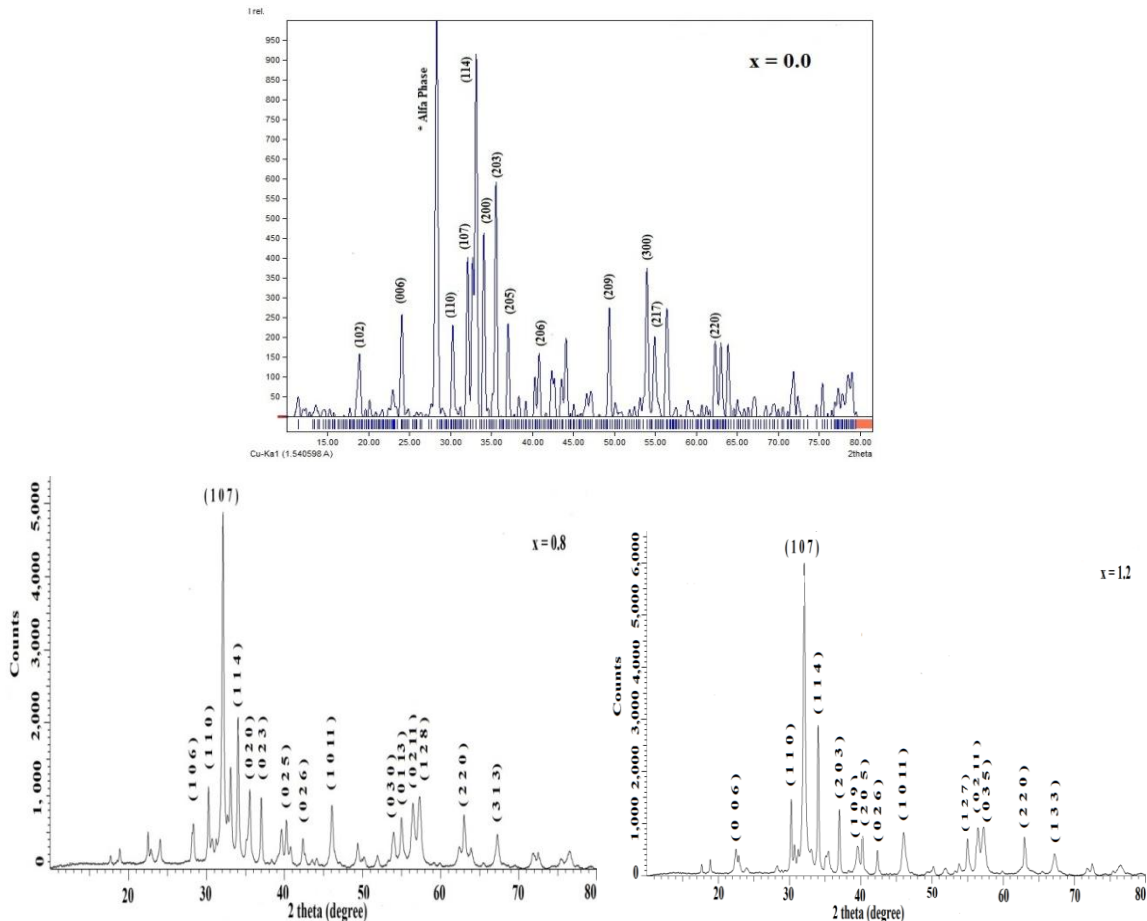


**Fig.1.X-ray diffraction patterns of  $\text{BaLa}_x\text{Fe}_{12-x}\text{O}_{19}$  nanohexaferrite**

2) *Microstructural Analysis*

Surface morphology of prepared samples was determined by Scanning Electron Microscopes. Fig. 3(a–d) shows the SEM micrographs with magnification 1  $\mu\text{m}$ , 100nm of the pure and  $\text{La}^{3+}$  substituted samples, sintered at  $800^\circ\text{C}$  in powdered form. We can see the grains are distributed homogenously without much agglomeration in  $\text{La}^{3+}$  substituted samples. Pure sample in Fig. 3(a) shows higher agglomeration.

Due to this, particles have tendency to form spherical shape. SEM images clearly show that Particle size by increasing the La ion substitution. It is due large ionic radius of La ion as compare to  $\text{Fe}^{3+}$  ion. In order to confirm the particle sizes are in nano range, TEM images was taken as shown in Fig. 4. Fig. 4(b) shows SAED images, which shows ring pattern means prepared ferrite have good crystallites and polycrystalline in nature.

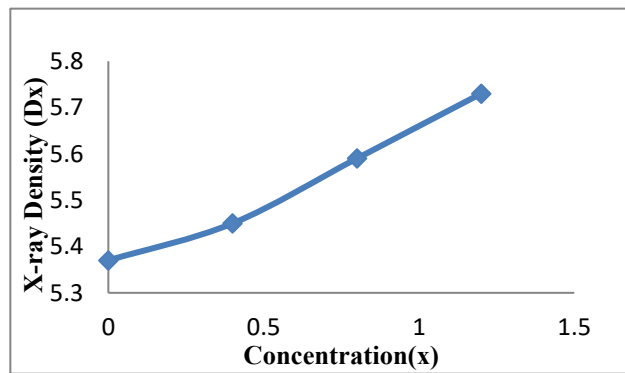
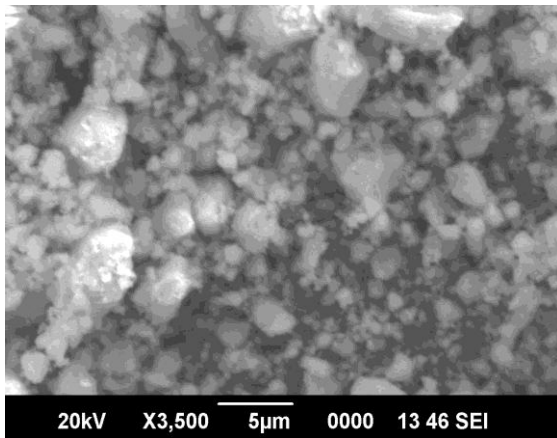
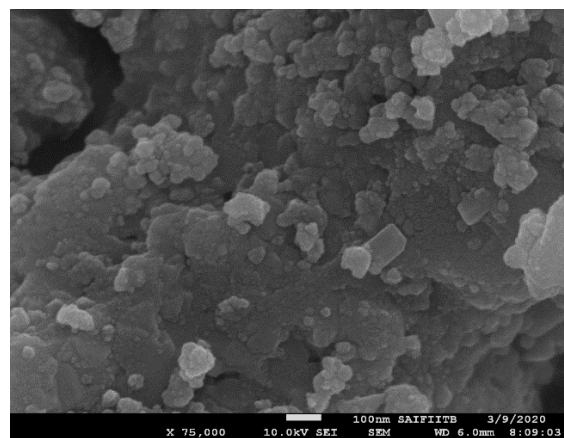


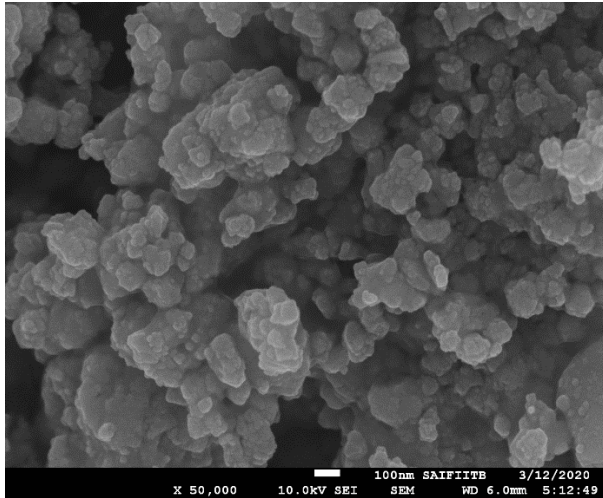
**Fig. 2. X-ray density versus concentration of  $\text{La}^{3+}$  ion**



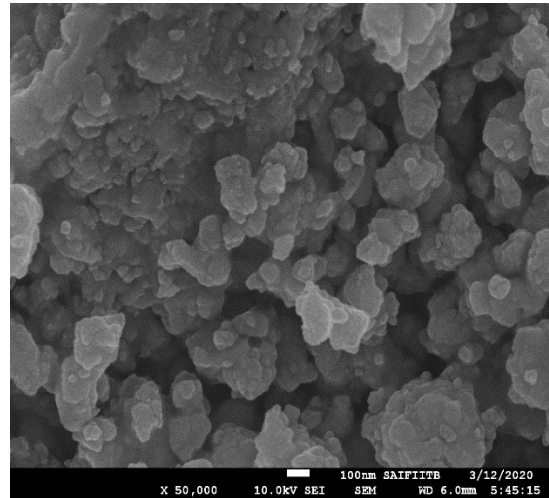
**(a)  $\text{BaFe}_{12}\text{O}_{19}$**



**(b)  $\text{BaLa}_{0.4}\text{Fe}_{11.6}\text{O}_{19}$**



(c)  $\text{BaLa}_{0.8}\text{Fe}_{11.2}\text{O}_{19}$



(d)  $\text{BaLa}_{1.2}\text{Fe}_{10.8}\text{O}_{19}$

Fig. 3. SEM micrographs (a-d) of prepared samples

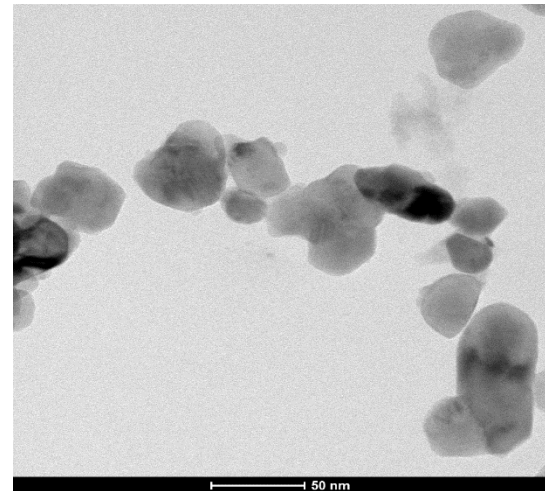
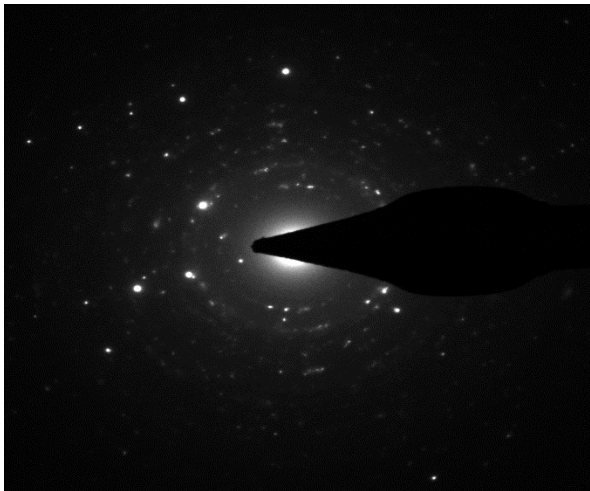


Fig.4. (a) SAED and (b) TEM images of sample

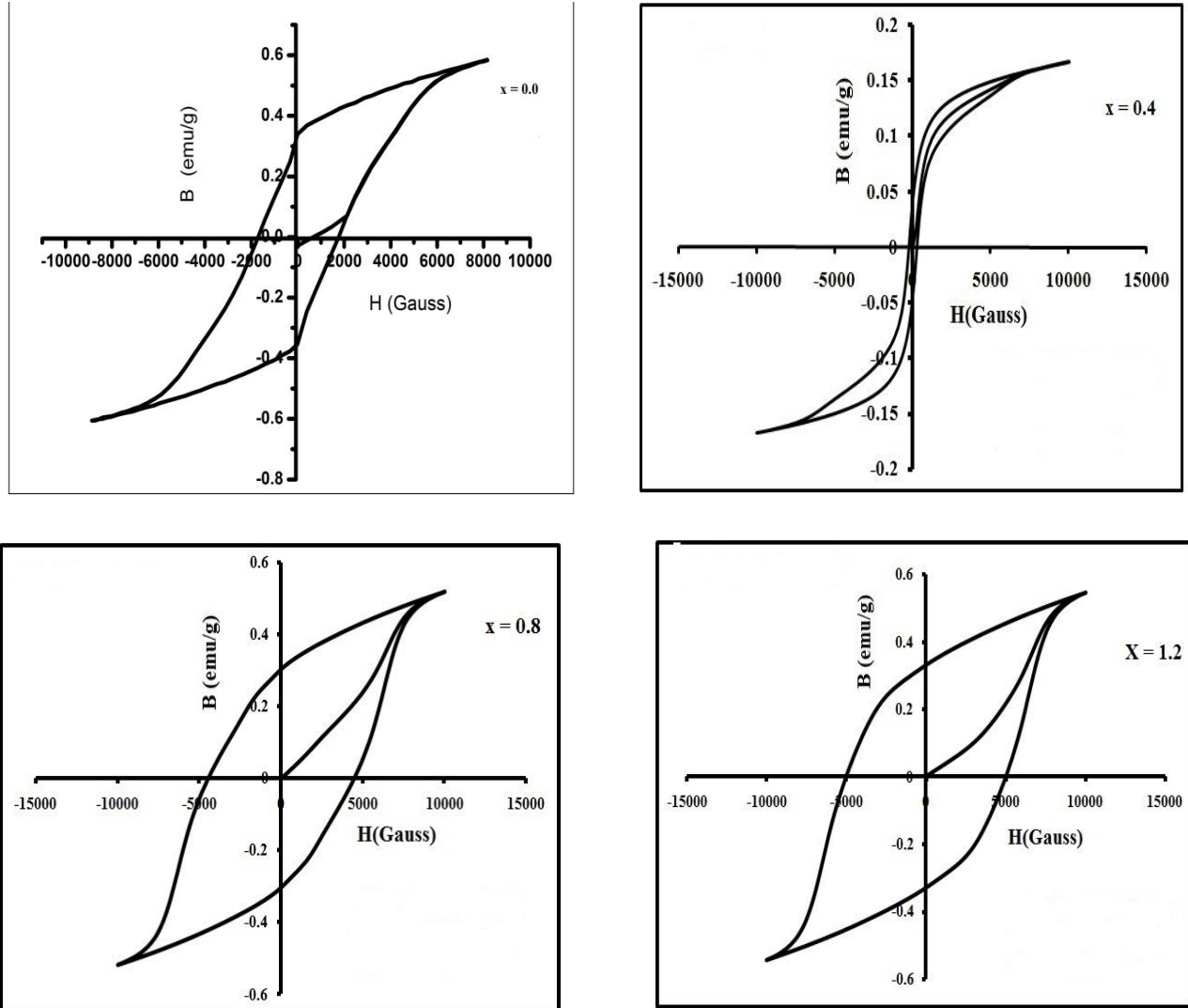


Fig.5. M-H curve for  $BaLa_xFe_{12-x}O_{19}$  ( $x = 0.0, 0.4, 0.8, 1.2$ ) samples at room temperature

Table 2.  
Magnetic parameters of prepared samples

Concentration (x)	Saturation Magnetization (Ms) emu/g ( $10^{-3}$ )	Coercivity (Hc) emu/g ( $10^{-3}$ )	Retentivity (Mr) ( $10^{-3}$ )	SQR Ratio
0.0	57.1	1737	36.9	0.646
0.4	16.56	200	5.62	0.339
0.8	51.92	4499	31.20	0.600
1.2	54.49	5000	33.97	0.6234

### B. Magnetic Properties

In order to investigate the magnetic properties of the prepared samples to applied external field, we measured magnetization values of samples at room temperature and results are shown in Fig.5. and respected values are given in table 2. The hysteresis loops of substituted hexaferrites show behaviour of the hard ferrite magnets with high coercive field ( $H_c$ ) as shown in Fig.5. The loops were broadened by  $La^{3+}$  substitution increases, showing an increase in coercivity. Fig. 5 shows that the  $M_s$  value of doped barium hexaferrites tend to increase as reported [15] which shows that increase in  $M_s$  can be correlated to the anisotropy as rare-earth ions are known to have large magneto-crystalline anisotropy and large magnetostriction. This behaviour of saturation magnetization occurred due to increase in hyperfine fields at 12k and 2b sub lattice sites or increase in  $Fe_3C-O-Fe_3C$  super exchange interactions, as observed in previous works [16-17] and spin canting [18] usually caused by rare earth ions. Coercivity value increases due to enhancement of the magneto crystalline anisotropy [19] with anisotropic  $Fe^{2+}$  ions locating on 2a site as usually found in rare earth ion substitutions.

Further, very high value of coercivity (5000 Gauss) was observed for  $x = 1.2$ . According to [20] materials used for longitudinal magnetic recording medium should have high coercivity (600 Oe) and if coercivity value above 1200 Oe, the materials are useful for the perpendicular recording media. So, in the present work, prepared Barium hexaferrites can be used in the perpendicular magnetic recording media.

### IV. CONCLUSIONS

Lanthanum substituted  $BaFe_{12}O_{19}$  nanohexaferrites were successfully synthesized via Sol-gel auto combustion technique. XRD confirms the hexagonal structure of  $La^{3+}$  substituted Barium hexaferrites which also confirmed by FTIR. SEM images also show hexagonal morphology of grains. TEM images shows prepared ferrite materials have nanosize particles. Magnetic properties analysis that the saturation magnetization is decreases, while the coercivity values are increases with the increase of  $La^{3+}$  ion substitutions. The value of Saturation magnetization and coercivity value obtained in the present work were found to be relatively high as compared to the values observed by other researchers. It is observed that these prepared nanohexaferrite materials can be used for permanent magnets, storage devices, recording media application.

### REFERENCES

- [1] Anjum Safia, Seher Amber & Mustafa Zeeshan, 2019. Effect of  $La^{3+}$  ion substituted M-type of barium hexaferrite on magnetic, optical and dielectric properties. *Applied Physics A*, 125,664.
- [2] Diepen, A.M. Van and Lotgering, F.K. 1974 .*J. Phys. Chem. Solids*, 35, 1641.
- [3] Jotania, R., Khomane, R., Chauhan, C., Menon, S., and Kulkarni, B., 2008. *J. Magn. Magn.Mater.* 320, 1095–1101.
- [4] Kumar, Gagan, Shah, Jyoti, Kotnala, R.K., Singh, Virender Pratap, Garg, Sarveena Godawari, Sagar E. Shirsath, Batoor, Khalid M. and Singh ,M., (2015). Super paramagnetic behaviour and evidence of weakening in super-exchange interactions with the substitution of  $Gd^{3+}$  ions in the Mg–Mn Nanoferrite matrix. *Mater.Res.Bull.* 63, 216–225.
- [5] Kaur, Talwindar, Kumar, Sachin, Bhat, Bilal H. and Srivastava, Ajeet Kumar,(2015).Enhancement in physical properties of Barium hexaferrite with substitution. *J. Mater. Res.* 65, 123-128.
- [6] Lechevallier, L., Breton, J.M. Le, Wang, J.F., and Harris, I.R., (2004) .*J. Magn. Mater.*, 269, 192.
- [7] Li, Cong-ju, Wang, Bin, & Wang, Jiao-Na, (2012). Magnetic and microwave absorbing properties of electrospun  $Ba_{1-x}La_xFe_{12}O_{19}$  nanofibers, *J. Mag.Mater.*, 324(7), 1305–1311.
- [8] Liu, X., Zhong, W., Yang, S., Yu, Z., Gu, B., & Du, Y. (2002). Structure and Magnetic Properties of  $La^{3+}$ -Substituted Strontium Hexaferrite Particles Prepared by Sol–Gel Method. *Phys. Status Solidi A*, 193, 314.
- [9] Liu, X., Zhong, W., Yang, S., Yu, Z., Gu, B., & Du, Y., *J. Magn.Mater.*, 238 (2002) 207.
- [10] Yang, Y., Liu, X., Jin, D. & Ma, Y.(2014). *Mater. Res. Bull.*, 59 37–41.
- [11] Ounnunkad, S. 2006. Improving magnetic properties of barium hexaferrites by La or Pr substitution. *Solid State Commun.* 138, 472–475.
- [12] Sauer, Ch., Kobler, U., Zinn, W., Stablein, H., (1978) *J. Phys. Chem. Solids*, 39, 1197
- [13] Shimada, M., and Magnetics, S., (1999). *IEEE Trans. Magn.*, 35, 3154.
- [14] Surig, C., Hempel, K. and Bonnenberg, D., (1994) *IEEE Trans. Magn.*, 30, 4092–4094.
- [15] Singh, Virender Pratap, Kumar, Gagan, Shah, Jyoti, Kumar, Arun, Dhiman, M., Kotnala, R.K., and Singh, M., (2015). Investigation of super-exchange interactions in  $BaHo_xFe_{12-x}O_{19}$  (0.1 to 0.4) nanohexaferrites and exploration at ultra high frequency region, *Ceram.Int.* 41(9), 1693–17101.
- [16] Singh, Virender Pratap, Kumar, Gagan, Kumar, Arun, Rai, Radhe Shyam, Valente, M.A.,(2016). Structural, Magnetic and Mossbauer study of  $BaLa_xFe_{12-x}O_{19}$  nanohexaferrites synthesized via Sol-gel auto combustion technique, *Ceramic International*, 42, 5011-5017.
- [17] Trukhanov, A.V., Trukhanov, S.V., Kostishin, V.G., Panina, L.V., Salem, M.M., Kazakevich, I.S., Turchenko, V.A., Kochervinskii, V.V. Krivchenya, D.A., (2017). Multiferroic properties and structural features of M-type Al-substituted barium hexaferrites. *Phys. Sol. State*, 59(4), 737–745.
- [18] Tyagi, S., Baskey, H.B., Agarwala, R.C., Agarwala, Shami, V. & T.C., (2011). *Ceram. Int.*, 37, 2631–2641.



**International Journal of Recent Development in Engineering and Technology**  
**Website: www.ijrdet.com (ISSN 2347-6435 (Online) Volume 15, Issue 03, March 2026)**

- [19] Trukhanov, S.V.,Trukhanov, A.V.,Kostishyn, V.G.,Panina, L.V.,Turchenko V.A., Kazakevich, I.S.,Trukhanov, A.V.,Trukhanova, E.L.,Natarov, V.O. & Balagurov, A.M.,(2017). Thermal evolution of exchange interactions in lightly doped barium hexaferrites. *J. Magn. Mater.*426, 554–562.
- [20] Trukhanov, S.V.,Trukhanov, A.V.,Kostishin, V.G.,Panina, L.V.,Kazakevich, I.S.,Turchenko, V.A. and Kochervinskiy, V.V.,(2016). Coexistence of spontaneous polarization and magnetization in substituted-type hexaferrites  $\text{BaFe}_{12-x}\text{Al}_x\text{O}_{19}$  ( $x \leq 1.2$ ) at room temperature. *JETP Lett.*103 (2), 100–105.
- [21] Yang, Y., Wang, F.,Shao, J., Huang, D., Trukhanov, A.,& Trukhanov, S.,(2019). *Appl. Phys. A: Mater. Sci. Process.*, 125, 37.